Optical Anisotropy in Films of Photoaddressable Polymers

V. Cimrová,*,†,‡ D. Neher,†,§ S. Kostromine,|| and Th. Bieringer||

Max-Planck-Institut für Polymerforschung, Ackermannweg 10, 55128 Mainz, Germany; Institute of Macromolecular Chemistry, Academy of Sciences of the Czech Republic, Heyrovsky Sq. 2, 162 06 Prague 6, Czech Republic; Institut für Physik, Universität Potsdam, Am Neuen Palais 10, 14469 Potsdam, Germany; and Bayer, 51368 Leverkusen, Germany

Received June 28, 1999; Revised Manuscript Received September 16, 1999

ABSTRACT: The photoinduced anisotropy in polymers and copolymers with a mesogenic and a nonmesogenic azobenzene moiety in the side chain were investigated. The results of the light-induced optical anisotropy study in thin films obtained by means of polarized UV−vis and IR absorption spectroscopy are presented. Starting from in-plane optically isotropic samples, irradiation with polarized laser at 514 nm induces significant and long-term stable optical anisotropy. The build-up of the optical anisotropy has been followed by transient absorption experiments with time resolution in the range of seconds. The coupling of photoinduced alignment between the two different azobenzenes could be proven by irradiation in the absorption band of the nonmesogenic chromophore. In- and out-of-plane refractive indices were determined using attenuated total reflection waveguide spectroscopy. High values of the in-plane light-induced birefringence of up to 0.23 depending on the relative content of the mesogenic and the nonmesogenic azobenzene moiety in polymer were found. The pronounced dependence of the birefringence on probe wavelength suggests a resonant enhancement of refractive index in the visible region. Refractive indices as a function of wavelength were evaluated from the measured polarized absorption spectra using the Kramers−Kronig relationship. Comparison with the results from waveguide spectroscopy showed that the anisotropy and dispersion of the refractive index below the absorption could almost entirely be explained by the reorientation of the two side-chain groups of the copolymer.

Introduction

Due to the growing demand in storage capacity, the interest in storage materials for different alternative optical storage applications has been continuously increasing in the past few years. For storing huge quantities of information, optical holographic recording, for example, is an attractive alternative to the more conventional magnetic technology. The main factor limiting large-scale manufacture of such systems is the lack of low-cost and easily processed recording materials. With the development of photorefractive crystals, this technology gained some momentum, and more recently, polymeric materials such as photorefractive polymers[1,2] and photopolymers[3,4] have emerged that can easily be processed into large-area films at low cost. The class of photoaddressable polymers is another supramolecular candidate for the list of potential recording media for optical as well as holographic recording. Photoaddressable polymers are in principle azobenzene-containing side-chain polymers. They have received increasing attention during the past decade due to their intriguing properties and a broad range of potential applications, especially in the field of optics and optoelectronics.[4−17] A leading motivation is the unique possibility of combining the functionality of conventional low-molar-mass liquid crystals with the properties of macromolecules. This is mainly possible due to the linking of different functional groups to the polymer main chain via flexible methylene spacer groups of varying length. For the materials under investigation, two functional groups are used: (1) chromophores, mostly azobenzene or derivatives of azobenzene as antenna for the incident light, and (2) mesogenic side groups. The task of the mesogenic side group is to follow the light-induced reorientation of the chromophores and to stabilize and amplify the new chromophore configuration (enhancement effect).

Irradiation with polarized light results in a uniaxial orientation of dye molecules: Light-induced isomerization cycles between the trans and cis configuration of the azo moiety provide a reorientation of the transition dipole of the chromophore into a direction perpendicular to the polarization vector of the incoming light. Chromophores with a dipole orientation perpendicular to the polarization direction will not take part in further excitations because the corresponding transition dipole momentum is equal to zero. The materials become birefringent with a light-induced optical axis parallel to the polarization direction of the actinic light.

An advantage of liquid crystalline side-chain polymers is the fact that the reorientation of the mesogenic side chains adjacent to the chromophore groups can be coupled with the reorientation of the dyes. The corresponding cooperative motion has mainly two effects. (1) The value of the light-induced birefringence is higher than in the case of orientation of the chromophores alone,and (2) the tendency of the mesogenic groups to align cooperatively in concert in a thermodynamic stable configuration can lead to a stable birefringence of the whole copolymer system.

The conditions for an effective coupling between the two functional groups is still an open question. Recently, Natansohn et al. published the results of IR measurements on a series of copolymers underlining the assumption that the dipolar interaction between the azo and the mesogenic groups is the most important factor for a cooperative reorientation in amorphous copolymers.[18] In liquid-crystalline systems, however, it can be

† Max-Planck-Institut für Polymerforschung.
‡ Academy of Sciences of the Czech Republic.
§ Universität Potsdam.
|| Bayer.

10.1021/ma991030t CCC: $18.00
Published on Web 11/20/1999

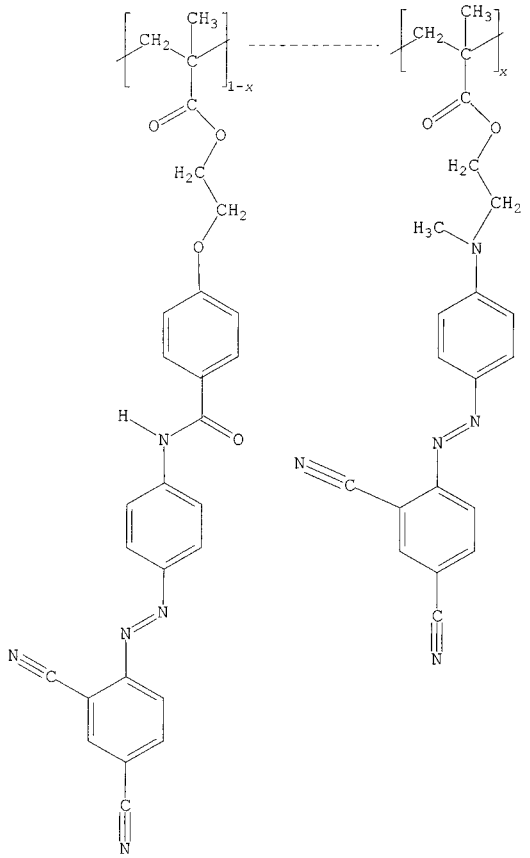

Polymer	x	T_g (°C)	Phase
K-0	0	149	LC 245 °C iso
K-10	0.1	149	LC 259 °C iso
K-20	0.2	148	LC 250 °C iso
K-30	0.3	148	LC iso
K-40	0.4	145	amorphous
K-100	1	129	amorphous

Figure 1. Structures of the polymers under study.

shown that even in the absence of dipolar coupling an orientation cooperatively can be induced.[19]

In this paper, we present spectroscopic measurements dealing with the problem of light-induced reorientation in azobenzene-containing copolymers. In these polymers, the strict distinction between light-absorbing chromophores and amplifying mesogens is lifted. The mesogen itself is an azobenzene chromophore with an additional phenyl ring, which evokes its liquid-crystalline character. From the practical point of view, this has the sizable advantage that the absorption of both functional groups lies in the visible region and can be followed by means of UV−vis spectroscopy. We will show that time-resolved polarization-dependent measurements could give a deep insight into the corresponding light-induced reorientation mechanisms.

Experimental Section

The polymers (see Figure 1) were synthesized by radical polymerization of monomeric methacrylates, which led to a degree of polymerization of about 100. Thin polymer films were prepared by spin-coating onto fused silica or glass substrates from tetrahydrofuran solutions. The optical quality of the films was good. Optical anisotropy was induced by irradiating the samples with linearly polarized light of argon laser at 514 nm (280−320 mW/cm^2). The photoinduced changes in absorption were investigated by two methods. In the first, samples have been illuminated continuously for a certain time, and polarized absorption spectra were then measured using a Perkin-Elmer

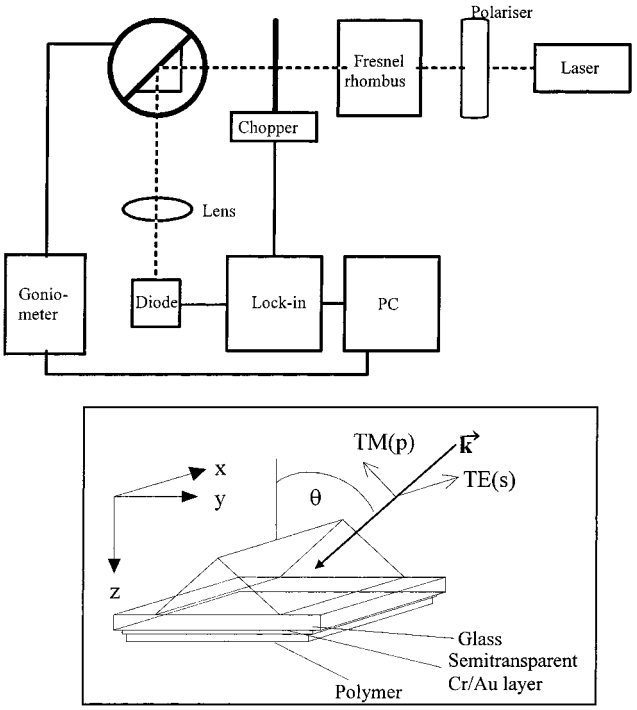

Figure 2. Experimental setup of the ATR method.

Lambda 9 spectrometer. The other approach was used to follow the kinetics of the anisotropy build-up. Samples were illuminated for 1 min. Then, the illumination was interrupted for 1 min to record polarized absorption spectra using a Hewlett-Packard UV−vis diode array spectrometer HP 8452A. This procedure was repeated up to a total light dose equal to that in the continuous illumination experiment. In both cases, absorption spectra were recorded with the probe light polarization either parallel ($A_{\parallel}$) or perpendicular ($A_{\perp}$) to the initial irradiating light polarization direction.

Attenuated total reflection (ATR) waveguide spectroscopy as a very powerful method was used to obtain complete information about in- and out-of-plane refractive indices of layer structures. Samples for ATR measurement were prepared by depositing a semitransparent thin gold electrode on a glass substrate, and the polymer films were subsequently spin-coated on top. If the layer thickness and polymer refractive index are sufficiently high, guided light can propagate parallel to the substrate plane. The resonance condition for the existence of those waveguide modes is[20]

$$k_{zm}d + \varphi_1 + \varphi_2 = m\pi \qquad (1)$$

where m is the order of the mode, k_{zm} is the normal component of the wave vector of mode m, d is the film thickness, and φ_1 and φ_2 are the phase shifts in reflection on the inner faces of the waveguide, which are given by Fresnel formulas and depend on light polarization. For thin layers, only plasmon surface polaritons (PSP) or surface plasmons can propagate along the metal−dielectric interface. In general, it is possible to excite two sets of waveguide modes: transverse electric (TE), which are sensitive to the in-plane refractive index n_x, and transverse magnetic (TM), which are sensitive to both the in-plane refractive index in the guided wave propagation direction n_y and out-of-plane refractive index n_z in the direction normal to the waveguide plane (see Figure 2).

To couple freely propagating light to PSPs or guided waves in polymer films, the sample was put in optical contact with a glass prism or half-sphere with the substrate facing the prism. The momentum of the exciting photon is increased by the index of refraction of the prism n_p in a way that coupling occurs at a well-defined incidence angle Θ_m. The coupling condition is fulfilled when the y-component k_{ym} of the wave vector of the guided mode m is equivalent to the projection of the incident

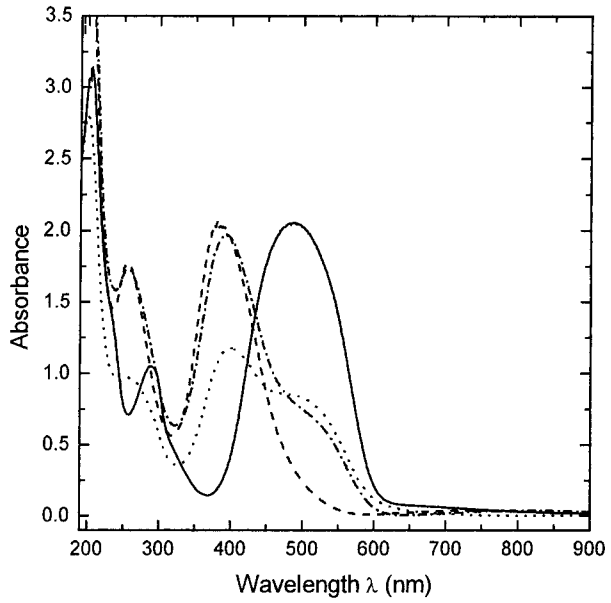

Figure 3. Absorption spectra of thin polymer films: K-0 (dashed), K-20 (dash-and-dot), K-40 (dotted), K-100 (solid line).

wave vector parallel to **y**:

$$k_{ym} = k_{\text{photon}} = n(w/c) \sin \Theta_m \qquad (2)$$

The mode spectrum was obtained by placing the substrate connected to the prism on a $\Theta - 2\Theta$ goniometer and recording the reflectivity by a photodiode for incidence angles ranging from 30° to 70°. The power of the probe laser was sufficiently low to avoid photoreaction in the sample. The ATR measurements were performed with probe light of 633, 690, and 780 nm. The experimental reflectivities curves were fitted by a computer program that calculates theoretical reflectivities of layered media using Fresnel's formulas. As a result, the thickness and the refractive indices in the three principal directions were obtained.

Results and Discussion

Absorption spectra of the neat polymers and copolymers are shown in Figure 3. Absorption maxima are located at 385 and 487 nm in neat homopolymers K-0 and K-100, respectively, corresponding to the absorption of the two different azobenzenes in side chain. For copolymers, contributions of both moieties are evident.

Before irradiation, identical absorption spectra were recorded for both mutually perpendicular polarization directions, demonstrating that films are initially in-plane optically isotropic. Polarized IR measurements also showed no in-plane anisotropy. After irradiation with the polarized light of an argon laser at 514 nm, an increase in absorption $A_\perp$ for light polarized perpendicular to the laser polarization direction and a decrease in absorption $A_\parallel$ were observed in homopolymer K-0 and all of the copolymers under study. This indicates the light-induced reorientation of the chromophores perpendicular to the laser polarization direction. An example for this generally observed behavior is shown in Figure 4 for copolymer K-20. Time evolution of the absorption using interrupted irradiation as described in the Experimental Section is shown in Figure 5. Note that the maximum of parallel absorption shifts to a longer wavelength. Its position corresponds to the maximum measured for the corresponding polymer solutions. Different local environments of the azobenzene side groups for both polarization directions could explain the shifts. Both azobenzene side-chain groups possess a large anisotropy of the polarizabilities $\Delta\alpha$ and large dipole moment μ (mesogenic $\Delta\alpha = 50.3$ Å^3 and μ

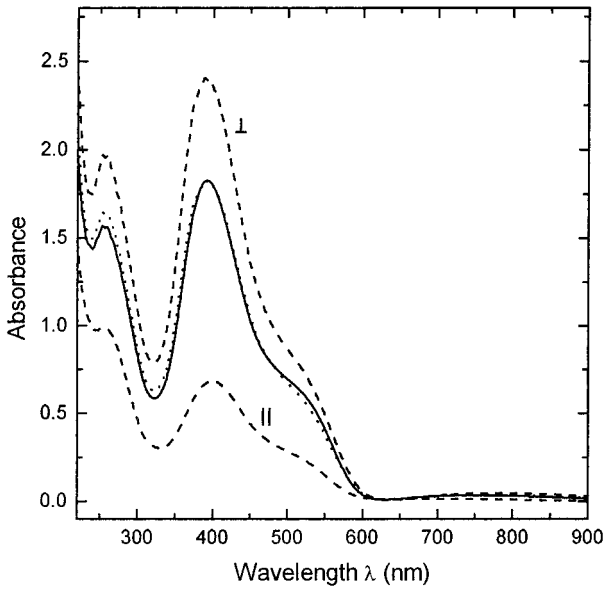

Figure 4. Polarized absorption spectra of thin film of K-20 before (solid) and after (dashed line) irradiation with polarized argon laser at 514 nm (light dose, 580 J/cm^2). The dotted curve shows average absorption calculated from the measured polarized spectra after irradiation.

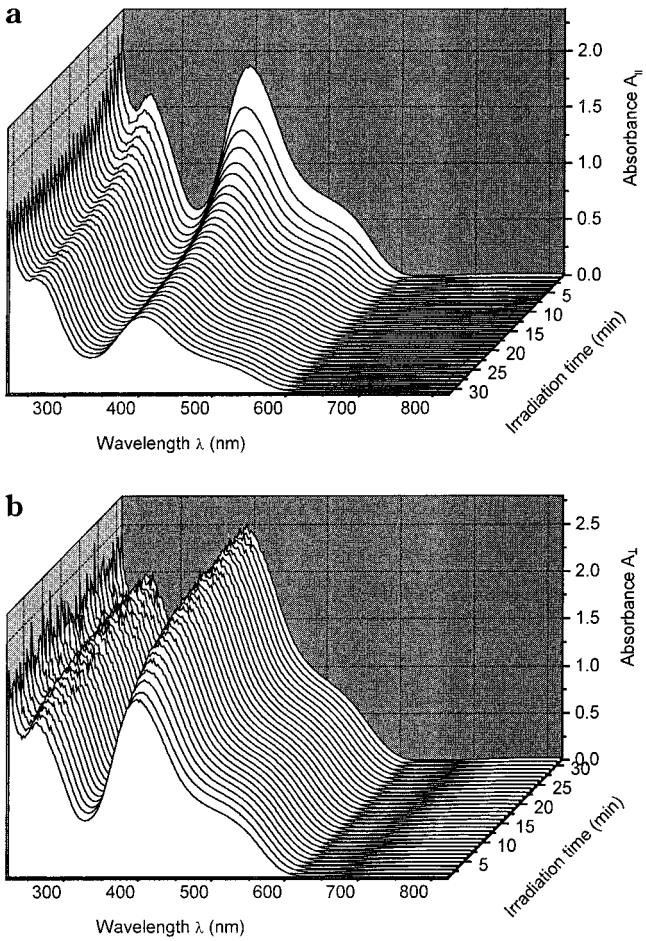

Figure 5. Polarized absorption spectra of thin film of K-20 during irradiation with polarized argon laser at 514 nm measured with polarization (a) parallel and (b) perpendicular to the laser polarization.

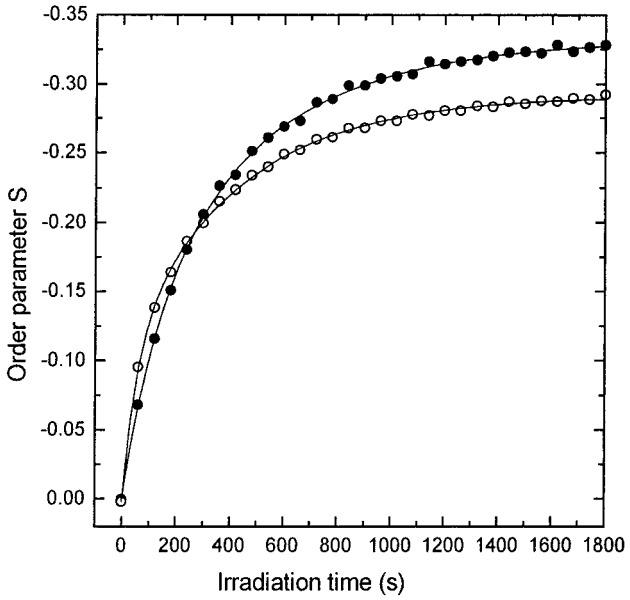

Figure 6. Time evolution of the order parameter S during irradiation with polarized argon laser at 514 nm for copolymer K-20. S was determined at the wavelengths of the absorption maximum of the mesogenic (384 nm, solid circles) and nonmesogenic (486 nm, open circles) chromophore.

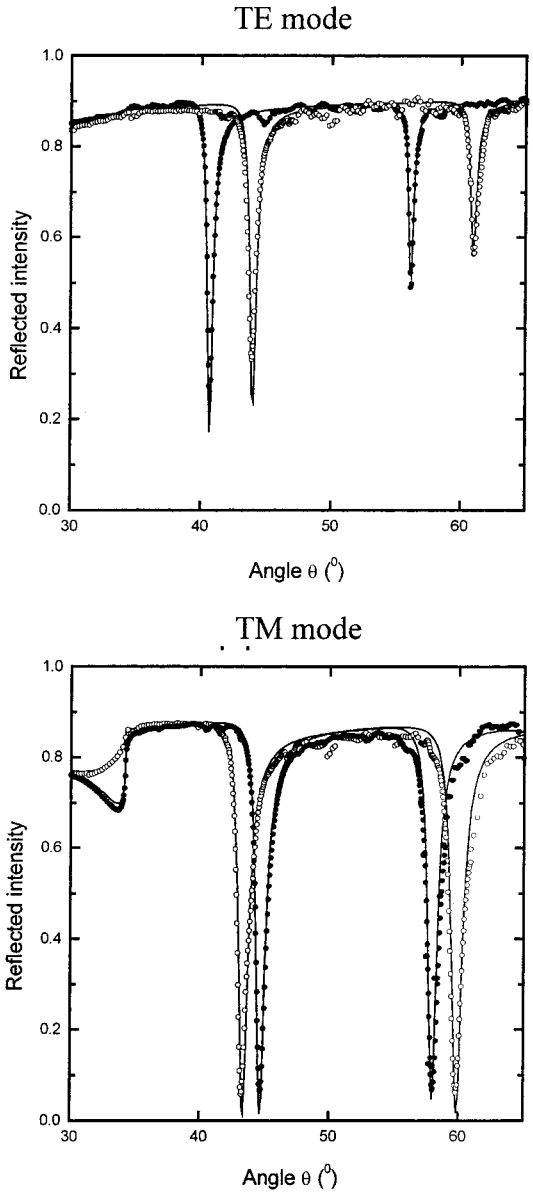

Figure 7. Reflectance spectra for TE and TM waveguide light mode measured on K-0 (glass/Au/K-0; $d = 785$ nm) before (solid circles) and after (open circles) irradiation with argon laser at 514 nm. Solid curves are best experimental fits calculated using Fresnel formulas. For the TE light mode, the polarization of the probe light was perpendicular to the argon laser polarization direction.

$= 7.8$ D, nonmesogenic $\Delta\alpha = 39.5$ Å^3 and $\mu = 8.9$ D[17]). It is well-known that the local electric field of the neighboring dipoles raises or lowers the absorption energy of the azobenzene group.[21,22] Parallel dipoles decrease and antiparallel dipoles increase the absorption energy. Reorientation of the chromophores perpendicular to the laser polarization gives rise to stronger intermolecular interactions, resulting in mutual shifts of both absorption maxima. Dielectric measurements showed that the dipoles prefer to align in an antiparallel fashion.[17]

After irradiation with polarized light of the same light dose, a decrease in both $A_\perp$ and $A_\parallel$ absorption was observed in polymer K-100 with the nonmesogenic azobenzene moiety only. Time-resolved absorption measurements on K-100 revealed an initial increase in perpendicular absorption $A_\perp$ followed by a continuous decrease in the absorption. This is indicative of either the photoinduced transition to a second stable conformation of the nonmesogenic chromophore or even photodegradation. After irradiation with the same light dose, only small changes in the average absorption were observed in K-0 and copolymers with low chromophore contents. This suggests that by irradiation at 514 nm no long-lived conformation changes take place in the mesogenic chromophore and only reorientation occurs. With the increasing content of the nonmesogenic chromophore, the average absorption decreases more significantly. The most pronounced changes were detected in neat polymer K-100. Similar behavior was observed in the IR absorption.

We have used the order parameter S, $S = <3\cos^2\theta - 1>/2$ as a measure of the degree of orientation order in the polymers. Here, θ is the angle between the long axis of the molecule relative to **x**, the direction of the light-induced optical axis (parallel to the direction of the laser polarization; the polarization plane is $x-z$). If the transition moment is oriented parallel to the molecular long axis, the order parameter is given by the relation $S = (R - 1)/(R + 2)$, where R is the dichroic ratio $R = A_\parallel/A_\perp$. For an ideal parallel and perpendicular orientation, $S = 1$ and $S = -0.5$, respectively, and $S = 0$ for the disordered state. In the polymers under study, the highest optical anisotropy was determined in the films of K-0 ($S = -0.36$), and the smallest anisotropy ($S = -0.155$) was found in the samples of K-100 after irradiation with the same light dose. The large anisotropy in K-0 proves that the mesogenic moiety can undergo efficient photoinduced reorientation by itself, even though the illumination is performed with a wavelength of the very tail of the absorption. It can be well expected that this process also occurs in the copolymer. In copolymers, at first reorientation or conformation changes in the nonmesogenic chromophore occur, followed by reorientation of the mesogenic unit. This is demonstrated in Figure 6, which shows the evolution of the order parameter as obtained by interrupted irradiation of copolymer K-20. For the same total light dose, the same order parameters were obtained

Table 1. Refractive Indices of the Polymers under Study Determined from ATR Measurement at Probe Wavelengths of 633 and 780 nm before and after Irradiation with Argon Laser at 514 nm[a]

	d	before irradiation			after irradiation			
polym	(nm)	n_{x0}	n_{y0}	n_{z0}	n_x	n_y	n_z	$n_y - n_x$
Probe Laser Beam at 633 nm								
K-0	580	1.726	1.726	1.631	1.602	1.828	1.666	0.226
	785	1.728	1.728	1.635	1.606	1.817	1.658	0.211
K-10	780	1.715	1.715	1.677	1.630	1.753	1.721	0.123
	988	1.715	1.715	1.681	1.626	1.783	1.718	0.157
K-20	555	1.764	1.764	1.665	1.628	1.852	1.710	0.224
K-30	656	1.783	1.783	1.673	1.640	1.874	1.746	0.234
K-40	580	1.780	1.780	1.694	1.649	1.880	1.772	0.231
K-100	560	1.844	1.844	1.783	1.778	1.836	1.810	0.058
Probe Laser Beam at 780 nm								
K-0	580	1.686	1.686	1.596	1.591	1.800	1.645	0.209
	785	1.703	1.703	1.602	1.597	1.779	1.655	0.182
K-10	780	1.675	1.675	1.643	1.606	1.715	1.694	0.109
	988	1.675	1.675	1.644	1.608	1.723	1.686	0.115
K-20	555	1.715	1.715	1.613	1.595	1.781	1.647	0.186
K-30	656	1.723	1.723	1.625	1.622	1.804	1.694	0.182
K-40	580	1.710	1.710	1.623	1.610	1.792	1.682	0.182
K-100	560	1.717	1.717	1.652	1.667	1.715	1.720	0.048

[a] Polarization plane, $x-z$; light dose, 580 J/cm^2.

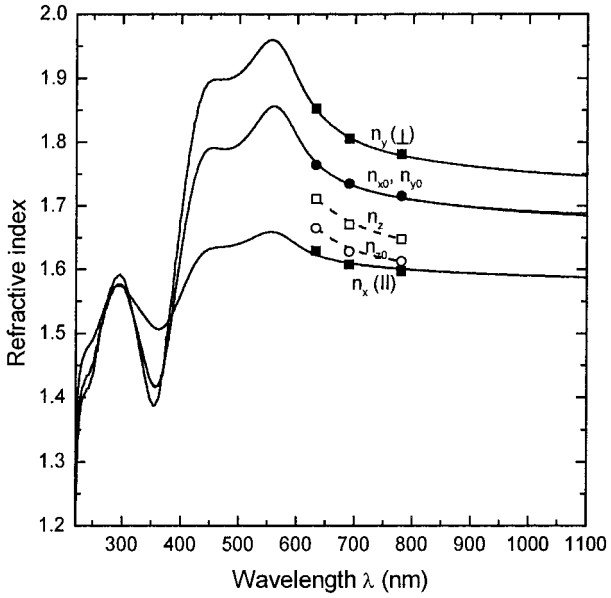

Figure 8. Refractive indices determined from ATR measurement before irradiation (in-plane n_{x0} and n_{y0}, solid circles; n_{z0}, open circles) and after irradiation with argon laser at 514 nm (light dose, 580 J/cm^2) (in-plane n_x and n_y, solid squares; n_z, open squares). Solid curves display the refractive index dispersion calculated from the measured absorption spectra.

by interrupted irradiation as in the case of the continuous one. This indicates an additive process with no back relaxation of the photoinduced anisotropy during the interruption of the irradiation. This benefit of our polymers is a result of the stabilizing influence of the mesogenic moieties.

Refractive indices in the three principal directions before and after polarized light irradiation were determined from ATR measurement. Typical reflectance spectra (TE and TM light mode) measured on the sample made from K-0 are shown in Figure 7. The results of the analysis of the measured ATR spectra for probe wavelength of 633 and 780 nm are summarized in Table 1 and displayed in Figures 8 and 9. Before irradiation, the same values of in-plane refractive indices (n_{x0}, n_{y0}) and lower values of the out-of-plane

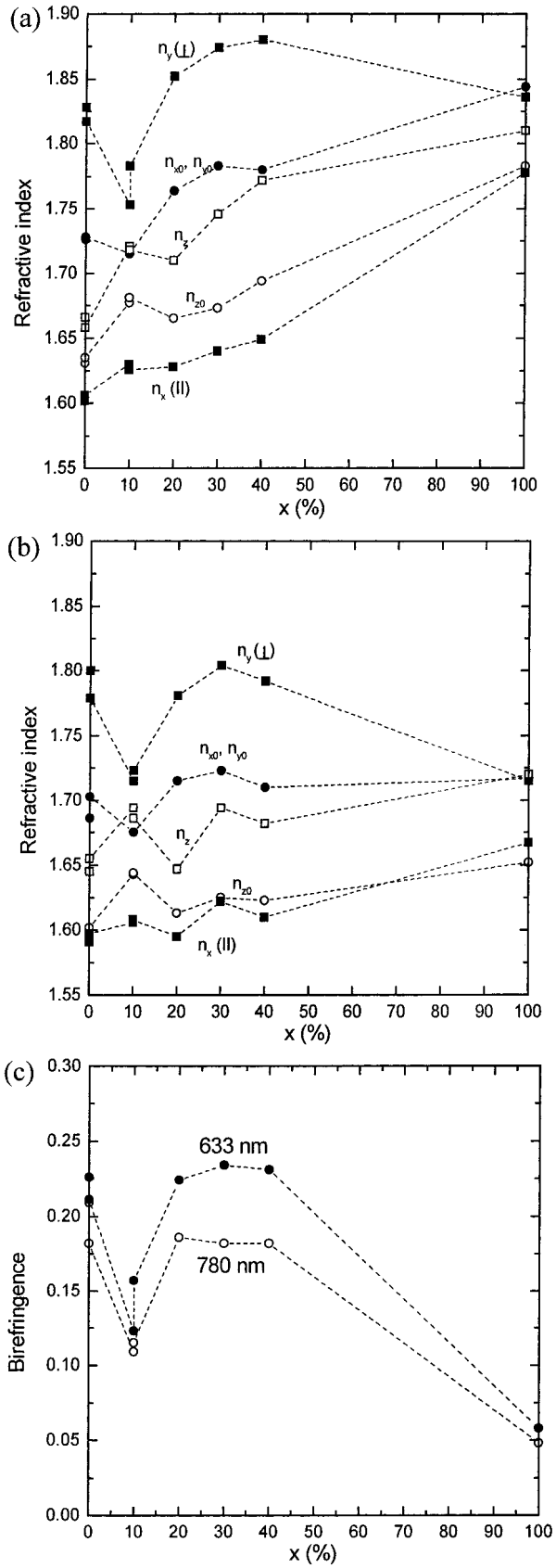

Figure 9. Refractive indices of polymers under study determined from ATR measurement at probe wavelengths of 633 (a) and 780 nm (b) before (circles) and after (squares) irradiation with argon laser at 514 nm (light dose, 580 J/cm^2) displayed as a function of the nonmesogenic chromophore content. (c) Birefringence ($B = n_y - n_x$) determined at probe wavelengths of 633 (solid circles) and 780 nm (open circles) displayed as a function of the nonmesogenic chromophore content.

refractive index were evaluated. This reveals initial out-of-plane anisotropy of thin films induced by the spin-coating process, long axes of the chromophores being preferentially oriented in the plane of the substrate rather than perpendicular. The values of in-plane refractive indices lie in the range 1.64−1.85, depending on the polymer structure and probe laser wavelength (see Figures 8 and 9). The clear rise in refractive index n for the shorter wavelength was observed, which indicates resonant enhancement (see Figure 8). As a consequence, the refractive index dependence on the structure for the probe laser beam wavelength of 780 nm, which is nearly out of the absorption for all of the polymers under study, is not so pronounced.

After the irradiation with polarized light, a birefringence is induced. In the homopolymer K-0 and all copolymers, refractive indices n_x (parallel to laser polarization direction) decreased and refractive indices n_y and n_z increased. A decrease in both in-plane refractive indices and an increase in the out-of-plane refractive index were detected in the polymer K-100. This result is in agreement with measured polarized absorption, where a decay of absorption in K-100 film was detected for both in-plane polarization directions after irradiation with the same light dose.

High values of the in-plane light-induced birefringence up to 0.23 were detected in polymer K-0 and copolymers K-20, K-30, and K-40. Lower values were detected in the copolymer K-10, and the lowest were found in polymer K-100. The lower birefringence in K-10 could be caused by a lower value of the out-of-plane anisotropy in K-10 given mainly by a higher value of out-of-plane refractive index. This indicates that a large amount of azobenzene side chains is oriented perpendicular to the film plane. Such chromophores are inactive in photoinduced processes. These results are in good agreement with the results obtained from absorption studies, where the absorption coefficient in the K-10 film determined in the absorption maximum of the mesogen chromophore is lower than that in the copolymers with lower mesogen contents.

The wavelength dependencies of refractive index and optical absorption are intimately related. We have calculated the refractive indices as a function of wavelength from polarized absorption spectra using the Kramers−Kronig formulas:

$$\epsilon'(\omega) = \epsilon_0 + \frac{2P}{\pi}\int_0^\infty \frac{x\epsilon''(x)}{x^2 - \omega^2}\,dx \qquad (3)$$

$$\epsilon''(\omega) = -\frac{2P}{\pi}\int_0^\infty \frac{\omega\epsilon'(x)}{x^2 - \omega^2}\,dx \qquad (4)$$

Here, ϵ' and ϵ'' are the real and imaginary parts, respectively, of the complex electric permittivity ϵ^*, which is related to the complex refractive index n^* by $\epsilon^* = (n^*)^2$, ϵ_0 is the background permittivity, and P denotes the principal value of the integrals. In the calculations, two main problems have to be taken into account. First, the whole absorption spectrum is not accessible to the common absorption spectroscopy in air. While the contribution of vibrational and rotational modes to n in the visible region is low, a main contribution to n arises from absorption in the UV wavelength range. It is meaningful to replace this contribution by a real parameter ϵ'_{UV}. Thus, one obtains the following relation:

$$\epsilon'(\omega) = \epsilon'_{UV} + \frac{2P}{\pi}\int_{\omega_{UV}}^{\omega_{IR}} \frac{x\epsilon''(x)}{x^2 - \omega^2}\,dx \qquad (5)$$

Here, ω_{UV} and ω_{IR} are the upper and lower optical frequencies covered by the polarized absorption spectroscopy.

A second problem arises from the fact that the absorption spectra of thin films on transparent substrates are usually corrected for the transmission of an uncovered substrate, neglecting reflection losses due to the additional polymer/glass interface as well as the wavelength dependence of the reflection loss at the air/polymer interface. We have used a scheme that takes into account the total transmission of the polymer/substrate system.[23] At first, a zero-order estimate of the imaginary part $\kappa_0(\lambda)$ of the complex refractive index is determined from the commonly corrected measured optical density. By use of a wavelength-independent refractive index, n_0, $\epsilon''_0(\lambda)$ is calculated. With eq 5 and ϵ'_{UV} set to a reasonable value (typically between 2 and 2.5), $\epsilon'_1(\lambda)$ is obtained by numerical integration. From this, the first-order dispersion $n_1(\lambda)$ is calculated using $\epsilon'_1(\lambda) = [n_1(\lambda)]^2 - [\kappa_0(\lambda)]^2$. By use of both $n_1(\lambda)$ and $\kappa_0(\lambda)$, the optical absorption of the total air/polymer/substrate/air-layered system is calculated using an optical transfer matrix approach[24] and corrected for the total absorption of the air/substrate/air system. If now the theoretical absorption at certain wavelengths exceeds the measured absorption, the corresponding values for $\kappa(\lambda)$ are reduced and vice versa, resulting in a corrected $\kappa_1(\lambda)$ as a measure of the intrinsic absorption of the polymer. Both $n_1(\lambda)$ and $\kappa_1(\lambda)$ are now used to calculate $\epsilon''_1(\lambda) = 2n_1(\lambda)\kappa_1(\lambda)$, and the numerical integration of eq 5 is performed to yield $\epsilon'_2(\lambda)$. This procedure is continued up to the point, where the changes in $n_i(\omega)$ and $\kappa_i(\omega)$ for subsequent iteration steps are smaller than a certain value. In this way, a consistent set of values for $n_i(\omega)$ and $\kappa_i(\omega)$ as a function of wavelength is obtained, which does explain the measured absorption of the sample and at the same time fulfils the Kramers−Kronig relationship.

In this approach, the only variable is ϵ'_{UV}. We have adjusted ϵ'_{UV} to give the best agreement between the experimental values for n and the calculated dispersion. A very good agreement with the results obtained from ATR measurements (see Figure 8) was found by using reasonable values for the background dielectric constant. The calculations also confirm that the pronounced wavelength dispersion in n and the large birefringence values at 633 nm are caused by resonant enhancement.

To check the validity of this approach, we have compared the intrinsic absorption of the polymer layer as determined from a line-width fit of the ATR spectra at a certain wavelength with the intrinsic absorption obtained by our iterative Kramers−Kronig approach. An example is shown in Figure 10 for a nonirradiated film of K-100. In-plane refractive indices evaluated from an ATR measurement at two measuring wavelengths (solid circles in Figure 10a) are in very good agreement with values of the refractive index dispersion calculated from the measured absorption spectrum using a reasonable value $\epsilon'_{UV} = 2.0$ (solid curve in Figure 10a). For the same value of ϵ'_{UV}, a very good agreement is found for the experimental and calculated values of the absorption coefficient for the two measuring wavelengths (Figure 10b). As an illustration, a calculated dispersion and an intrinsic absorption using a too-high value of $\epsilon'_{UV} = 2.3$

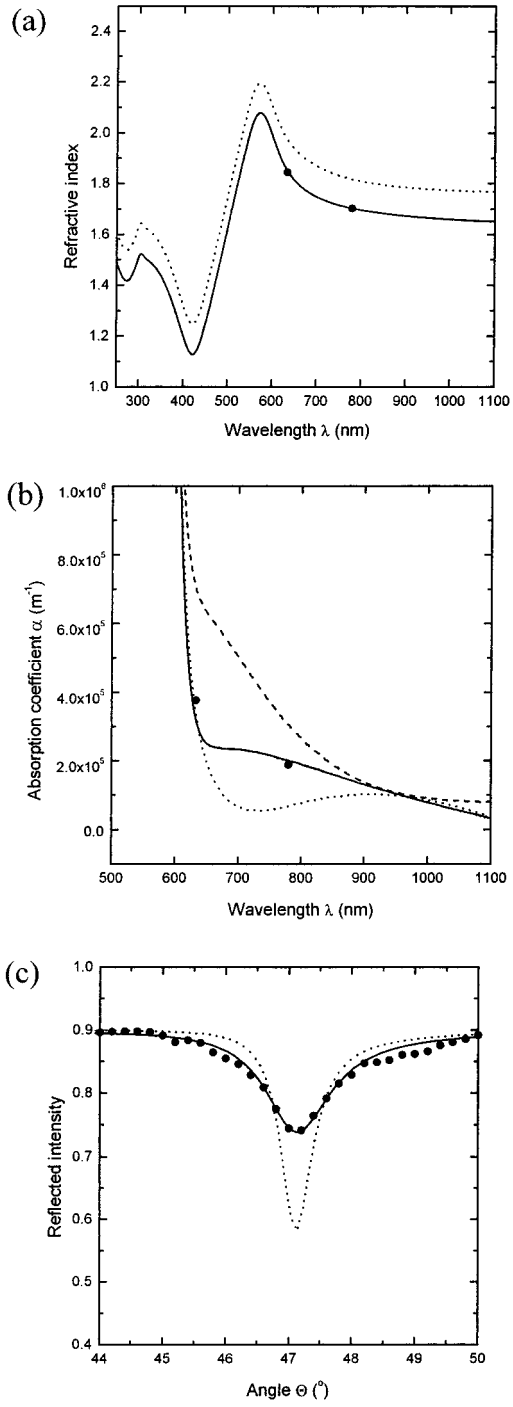

Figure 10. In-plane refractive indices (a) and absorption coefficients (b) of nonirradiated K-100 evaluated from ATR measurement (solid circles) and refractive index dispersion (a) and intrinsic absorption (b) calculated from the measured absorption spectrum of a K-100 film using the Kramers−Kronig relationship with two different values of background dielectric constant $\epsilon'_{UV} = 2.0$ (solid curve) and $\epsilon'_{UV} = 2.3$ (dotted curve). The dashed curve shows the measured absorption. (c) Measured reflectivity in the TE-mode (solid circles) at the probe laser beam wavelength of 780 nm and theoretical fit (solid curve) to the measured data giving the value of refractive index in (a) and absorption coefficient in (b). The dotted curve is a theoretical curve calculated with the lower absorption coefficient corresponding to the higher $\epsilon'_{UV} = 2.3$.

(dotted curves) are shown. This higher value of ϵ'_{UV} gives a line-width in the ATR spectrum (dotted curve in Figure 10c) much narrower than the measured one. The dashed curve in Figure 10b displays the measured absorption coefficient, which is higher in the tail of the absorption than is the intrinsic one (solid curve). Hence, the procedure confirms that a large fraction of the absorption measured in transmission in the tail of the absorption originates from reflection losses. The good correspondence of the calculated and measured refractive indices proves that the anisotropy and dispersion of the refractive index below the absorption can almost entirely be explained by the anisotropy in optical absorption caused by reorientation of the azobenzene units.

Table 2. Refractive Indices of Copolymer K-20 (d = 555 nm) Determined from ATR Measurement at Probe Wavelengths of 633 and 780 nm before and after Irradiation with Argon Laser at 514 nm[a] and after 5 Months of Relaxation

	633 nm			780 nm			
	n_x	n_y	n_z	n_x	n_y	n_z	$n_y - n_x$
before irrad	1.764	1.764	1.665	1.715	1.715	1.613	0
after irrad	1.628	1.852	1.710	1.595	1.781	1.647	0.186
after 5 months	1.628	1.852	1.712	1.603	1.792	1.675	0.189

[a] Polarization plane, $x-z$; light dose, 580 J/cm^2.

A thermal back relaxation at room temperature was not observed for more than 5 months. The values of refractive indices measured after this period are displayed in Table 2 for copolymer K-20. The enhanced birefringence is attributed to a cooperative motion of side chains. This fact could be proved by measurements of photoinduced birefringence as a function of the laser irradiation intensity. The influence of the laser irradiation wavelength on the reorientation process of azobenzene side-chain groups will be discussed in a forthcoming paper.

Conclusion

Initially, in-plane optically isotropic films of polymers and copolymers with mesogenic and nonmesogenic azobenzene moieties exhibited optical anisotropy and high values of the birefringence with long-term stability after irradiation with a polarized laser at 514 nm at room temperature. In- and out-of-plane refractive indices were determined using waveguide spectroscopy. The evaluation of the refractive indices in all three principal directions revealed the initial out-of-plane anisotropy of thin films induced by the spin-coating process. A dependence of birefringence on the relative content of side-chain moieties and on the laser probe wavelength was found. On the basis of our calculation of the refractive index dispersion using the Kramers−Kronig relationship, we have proved that the highest values of the birefringence up to 0.23, as measured with a probe laser beam at 633 nm, are caused by a resonant enhancement of the refractive index in the visible region. The calculations also confirm that the anisotropy and dispersion of the refractive index below the absorption could almost entirely be explained by the reorientation of the two side-chain groups of the copolymer. Transient absorption experiments showed a coupling of the photoinduced alignment between the two different azobenzenes moieties. No back relaxation of the photoinduced anisotropy during the interruption of the irradiation occurred.

Acknowledgment. We thank Professor G. Wegner for his support and discussion and J. Worm for the

programs for evaluation of refractive indices from ATR spectra.

References and Notes

(1) Meerholz, K.; Volodin, B. L.; Sandalphon; Kippelen, B.; Peyghambarian, N. *Nature* **1994**, *371*, 497.
(2) Volodin, B.; Meerholz, K.; Sandalphon; Kippelen, B.; Peyghambarian, N. *Proc. SPIE-Int. Soc. Opt. Eng.* **1994**, *2144*, 72.
(3) Gambogi, W. J.; Weber, A. M.; Trout, T. J. *Proc. SPIE-Int. Soc. Opt. Eng.* **1993**, *2043*, 2.
(4) Waldman, D. A.; et al. *J. Imag. Sci. Technol.* **1993**, *41*, 497.
(5) Todorov, T.; Nikolova, L.; Tomova, N. *Appl. Opt.* **1984**, *23*, 4309.
(6) Eich, M.; Wendorf, J. H. *J. Opt. Soc. Am. B* **1990**, *7*, 1428.
(7) Wiesner, U.; Reynolds, N.; Boeffel, CH.; Spies, H. W. *Liq. Cryst.* **1992**, *11*, 251.
(8) Stumpe, J.; Muller, L.; Kreysig, D. *Makromol. Chem., Rapid Commun.* **1991**, *12*, 81.
(9) Natansohn, A.; Rochon, P.; Gosselin, J.; Xie, S. *Macromolecules* **1992**, *25*, 2268.
(10) Ramanujam, P. S.; Holme, N. C. R.; Hvilsted, S. *Appl. Phys. Lett.* **1996**, *68*, 1329.
(11) Tripathy, S.; Dong; Yu-K.; Lian, Li; Kumar, J. *Pure Appl. Chem.* **1998**, *70*, 1267.
(12) Labarthet, L. F.; Sourisseau, C. *J. Raman Spectrosc.* **1996**, *27*, 491.
(13) Dumont, M.; Froc, G.; Hosotte, S. *Nonlinear Opt.* **1995**, *9*, 327.
(14) Ikeda, T.; Horiuchi, S.; Karanjit, Durga, B.; Kurihara, S.; Tazuke, S. *Macromolecules* **1990**, *23*, 36.
(15) Kawanishi, Y.; Tamaki, T.; Seki, T.; Sakuragi, M.; Ichimura, K. *Mol. Cryst. Liq. Cryst.* **1992**, *218*, 153.
(16) Bieringer, T.; Wuttke, R.; Haarer, D. *Macromol. Chem. Phys.* **1995**, *196*, 1375.
(17) Zilker, S. J.; Bieringer, T.; Haarer, D.; Stein, R. S.; van Egmond, J. W.; Kostromine, S. G. *Adv. Mater.* **1998**, *10*, 855.
(18) Natansohn, A.; Rochon, P.; Meng, X.; Barrett, C.; Buffeteau, T.; Bonenfant, S.; Pezolet, M. *Macromolecules* **1998**, *31*, 1155.
(19) Läsker, L.; Fischer, T.; Stumpe, J.; Kostromin, S.; Ivanov, S.; Shibaev, V.; Ruhmann, R. *Mol. Cryst. Liq. Cryst.* **1994**, *253*, 1.
(20) Tien, P. K. *Rev. Mod. Phys.* **1977**, *49*, 361.
(21) Brown, D.; Natansohn, A.; Rochon, P. *Macromolecules* **1995**, *28*, 6116.
(22) Meng, X.; Natansohn, A.; Barrett, C.; Rochon, P. *Macromolecules* **1996**, *29*, 946.
(23) Neher, D.; Kaltbeitzel, A.; Wolf, A.; Bubeck, C.; Wegner, G. *J. Phys. D: Appl. Phys.* **1991**, *24*, 1193.
(24) Cimrová, V.; Neher, D. *J. Appl. Phys.* **1996**, *79*, 3299.

MA991030T